Available online at www.sciencedirect.com
ScienceDirect
Dyes and Pigments 77 (2008) 153–157
DYES and PIGMENTS
www.elsevier.com/locate/dyepig

UV–visible, fluorescence and EPR properties of porphyrins and metalloporphyrins

Wenqi Zheng, Ning Shan, Lianxiang Yu, Xingqiao Wang*

College of Chemistry, Jilin University, Changchun 130021, PR China

Received 25 December 2006; received in revised form 15 April 2007; accepted 17 April 2007
Available online 13 May 2007

Abstract

In order to search for novel luminescent and EPR oximetry materials, a series of porphyrins and metalloporphyrins with different peripheral substitutes and central transition metal ions were synthesized and their UV–vis, fluorescence and EPR spectra were studied. It was found that variations in the peripheral substituents imparted no change to the UV–vis spectra in the case of metal-free porphyrins. However, differences in the central transition metal ions resulted in changes in the energy of electron transitions which caused changes in UV–vis spectra. Variations in the peripheral substituents and the central metal ions influenced both the fluorescence and EPR spectra.

Keywords: Porphyrins; Metalloporphyrins; UV–vis, fluorescence and EPR properties

1. Introduction

Porphyrins, metalloporphyrins and related molecules have received a great deal of attention in recent years because they display interesting photophysical, photochemical and electrochemical properties. Porphyrins play very important roles in essential biological activities such as photosynthesis [1,2] and participate in oxygen transport as hemoproteins [3]. They enjoy application in many fields, such as photodynamic therapy [4–5], molecular wires [6–9], light-energy conversion [10–13], third-order nonlinear optical materials [14–16] and fluorescence switches [17]. In recent years the measurements of oxygen *in vivo* using EPR techniques have been developed [18].

Porphyrins are a type of macrocyclic organic molecule which have an extensive system of delocalized π electrons. They can be modified by connecting different peripheral substitutes, changing the central metal or expanding the size of the macrocycle. In this paper, a series of porphyrins and metalloporphyrins with different peripheral substitutes and central transition metals were synthesized. The influence of both the peripheral substituents and the central metal ions on the UV–vis, fluorescence and EPR properties of the synthesized compounds was determined. The work presented may be of use in the synthesis of novel luminescent and EPR oximetry materials.

2. Experimental

2.1. Apparatus and measurements

UV–vis spectra were recorded on a Cintra 10e UV–visible spectrophotometer; fluorescence spectra were acquired using a Perkin Elmer LS55 Fluorescence spectrometer, employing a 500 W Hg–Xe high pressure lamp. Fluorescence quantum yields were measured using tetraphenylporphyrin zinc as standard ($\Phi = 0.033$) [19]. The UV–vis and fluorescence spectra of the porphyrin compounds were measured in chloroform solution at $\sim 10^{-6}$ M. Electron paramagnetic resonance signals were recorded on a JES-FE3AX ESR spectrometer; all measurements were carried out using solid samples;

* Corresponding author.
E-mail address: wangxingqiao@mail.jlu.edu.cn (X. Wang).

0143-7208/$ - see front matter © 2007 Elsevier Ltd. All rights reserved.
doi:10.1016/j.dyepig.2007.04.007

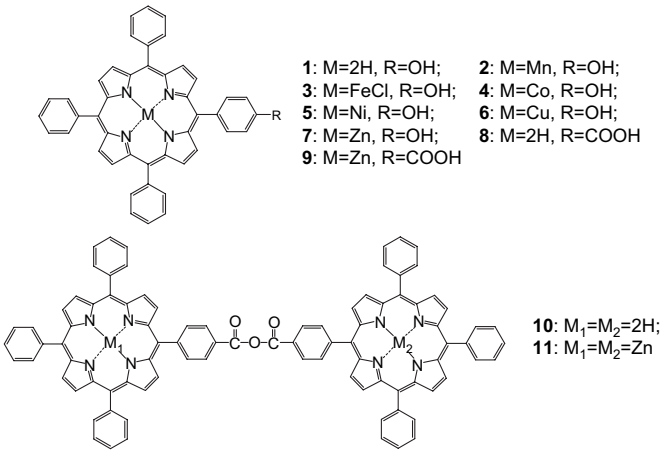

Fig. 1. The structures of the porphyrin compounds synthesized.

frequency: 100 kHz, microwave power: 9.44 GHz and time constant: 0.03 s. Matrix-assisted laser desorption ionization time-of-flight mass spectrometry (MALDI-TOF-MS) was estimated using an Axima CRR spectrometer.

2.2. Syntheses of porphyrins and metalloporphyrins

Both the structures of the porphyrins and metalloporphyrins synthesized are shown in Fig. 1. Compounds **1** and **10** were synthesized as described previously [20,21]and **8** and **9** as described in Ref. [22]. Compounds **2**–**7** were synthesized according to the known procedure [23]. Compound **11** was synthesized as follows: A solution of 200 mg of porphyrin **10** in 100 ml dried dichloromethane was stirred in an ice and salt bath for 20 min and the ensuing solution was stirred at −5 °C for 12 h after the addition of 100 mg of dicyclohexylcarbodiimide. After filtration under vacuum the crude product was concentrated and then purified via column chromatography by (100–200 mesh silica gel) eluting with dichloromethane. The first fraction was the desired product of compound **11**; MALDI-TOF MS, *m/z*: 1425.5.

3. Results and discussion

3.1. UV–vis spectra

The absorption spectra of the metal-free porphyrins **1**, **8** and **10** showed a typical Soret band and four Q bands (Fig. 2a) and the positions of their absorption peaks were identical. The band at 420 nm was assigned to the Soret band arising from the transition of $a_{1u}(\pi)$–$e_g^*(\pi)$, and the other four absorption maxima (515, 550, 590 and 650 nm) were attributed to the Q bands corresponding to the $a_{2u}(\pi)$–$e_g^*(\pi)$ transition. The different peripheral substituents did not change the transition mode of the porphyrin molecules.

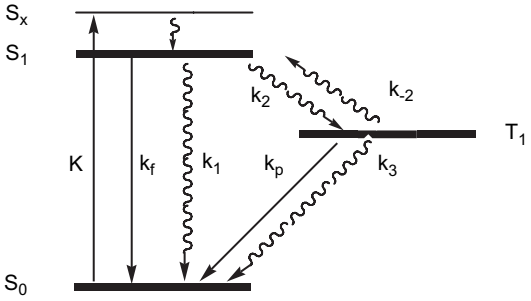

Fig. 3. Decay scheme for singlet and triplet relaxation. The radiation processes are shown as straight lines; the radiationless processes are shown by wave lines.

In general, the central part of the metalloporphyrin ring is occupied by a metal ion linked to a pyrrole ring. The metal ion accepts the lone-pair-electrons of the N atoms of the pyrrole rings, while electrons of the metal ion are donated to the porphyrin molecule, forming delocalized π bonds, which permit the easy flow of electrons within the delocalized π system. It can be seen in Fig. 2b and c that the UV–vis spectra of the metalloporphyrins exhibited one Soret band and either one or two Q bands; the small number of Q bands is typical of metalloporphyrins. When the metal ion coordinates with the N atoms, the symmetry of the molecule increases and the number of Q bands therefore decreases. For Co, Ni and Cu porphyrins, their delocalized π bonds decreased the average electron density of the metalloporphyrins which increased the energy available for electron transition as a result, a blue shift of the Soret bands occurred. However the delocalized π bands of the Mn(II) and Zn(II) porphyrins increased the average electron density of the porphyrin, which lowered the energy for electron transition, leading to a red shift in the Soret band.

3.2. Fluorescence spectra

Fig. 3 shows an energy level diagram that describes the emission from most aromatic molecules with singlet ground

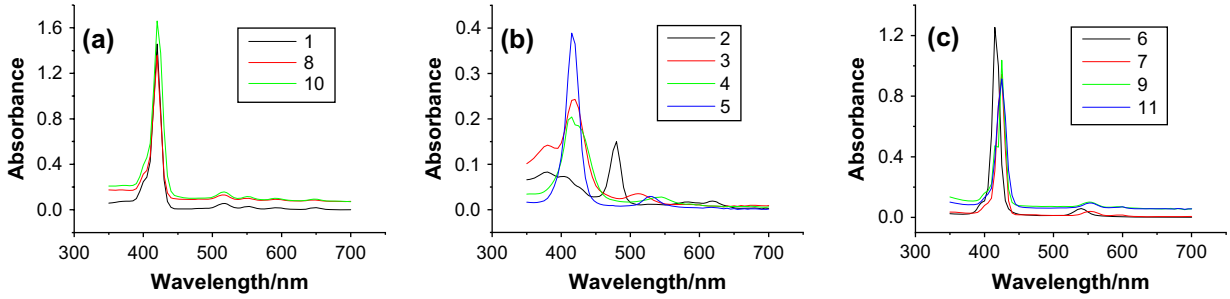

Fig. 2. UV–vis spectra of porphyrin compounds.

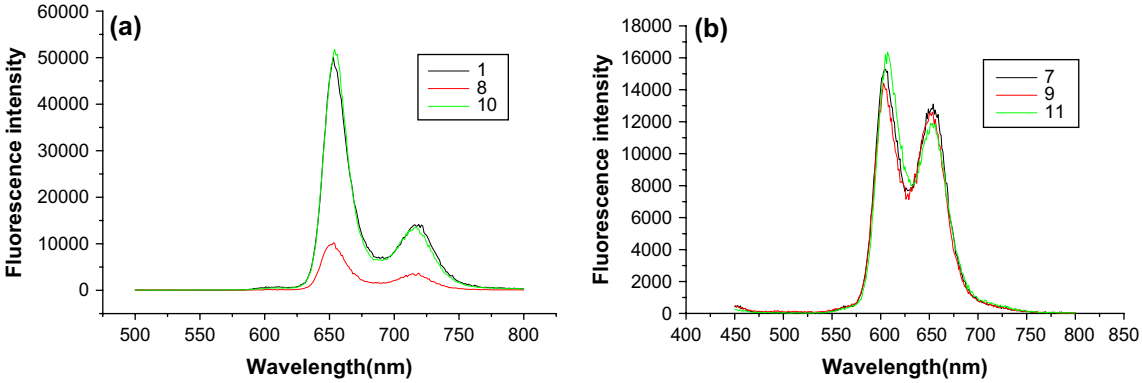

Fig. 4. Fluorescence spectra of porphyrin compounds.

states. Excitation from the ground state S_0 to any singlet excited state S_x leads to very fast radiationless decay to the lowest excited singlet S_1. From S_1 the molecule can emit fluorescence radiation $S_1 \rightarrow S_0$ at the rate k_f, can radiationlessly decay S_1 S_0 at the rate k_1, or can internally convert to the lowest triplet $S_1 \rightarrow T_1$ at the rate k_2. S_1 decays between 10^{-12} and 10^{-7} s, after which, if the system is still excited, it exists in the lowest triplet form T_1. The molecule can emit phosphorescent radiation $T_1 \rightarrow S_0$ at the rate k_p from T_1, can radiationless decay $T_1 \rightarrow S_0$ at the rate k_3, or can be excited again to the first excited singlet $T_1 \rightarrow S_1$ at the rate k_{-2}. Thus, only the relaxation process from S_1 to S_0 with rate k_f can emit fluorescent radiation.

The fluorescence spectra of the metal-free porphyrins and metalloporphyrins are shown in Fig. 4; fluorescence signals had not been detected for metalloporphyrins **2**–**6** under the particular experimental conditions used. The relevant fluorescence and quantum yields are shown in Table 1.

The order of the fluorescence intensity of the porphyrins was **10** > **1** > **11** > **7** > **9** > **8**. From Fig. 4a it can be seen that the metal-free porphyrins displayed two emission peaks at ~650 and 720 nm. Comparing **1** with **8**, the electron-donating hydroxyl group in **1** resulted in an increase in the average electron density of the conjugated porphyrin system; the transition in **1** was $\pi \rightarrow \pi_1^*$. However, the electron-withdrawing carboxyl group in **8** resulted in a decrease in the average electron density of the conjugated porphyrin system. The $n \rightarrow \pi_1^*$ transition of **8** was forbidden and the lowest excited singlet state S_1 was of the n, π_1^* type. The intersystem crossing (ISC) of $S_1 \rightarrow T_1$ was intensified which resulted in the fluorescence intensity weakening in **8**. It is evident from Fig. 5 that the energy band gap from $S_{\pi,\pi 1^*}$ to $T_{\pi,\pi 1^*}$ was larger than that from $S_{n,\pi 1^*}$ to $T_{n,\pi 1^*}$. The transition from $S_{n,\pi 1^*}$ to T_{n,π^*} via ISC was more easily accomplished than from $S_{\pi,\pi 1^*}$ to $T_{\pi,\pi 1^*}$. Hence, the fluorescence intensity of **1** was much stronger than that of **8**. The fluorescence intensity of **10** was the strongest of all the synthesized porphyrin compounds, being almost five times greater than that of the corresponding monomer **8**, indicating that there was efficient S_1–S_1 energy transfer between the two porphyrin moieties. Intramolecular singlet, excited state, energy transfer overlaps the two molecular orbitals of **10**, so this kind of direct energy transfer was considered to be possible as reported by Dexter [24]. Bisphenyl acid anhydride at the meso and meso′ positions of **10** resulted in enhancement of the intramolecular S_1–S_1 energy transfer so that **10** showed the strongest fluorescence radiation of all of the porphyrin compounds.

Of the metalloporphyrins, only the zinc porphyrins emitted fluorescence; the order of fluorescence intensity of the zinc porphyrins was 11 > 7 > 9 (Fig. 4b). The emission peaks were situated at ~600 and 650 nm which were some 50 nm blue shifted compared to the metal-free porphyrins. The fluorescence intensities of **7** and **11** were much weaker than those of the corresponding metal-free porphyrins **1** and **10** because zinc weakened the fluorescence radiation.

Table 1
Data of UV–vis and fluorescence spectra of porphyrin compounds

Compounds	Absorption (λ_{max}/nm)		Fluorescence (λ_{em}/nm)	Φ
	Soret band	Q band		
1	420	515, 550, 590, 650	653, 719	0.207
2	480	585, 620		
3	420	514		
4	415	545		
5	415	530		
6	415	540		
7	425	555	604, 654	0.176
8	420	515, 550, 590, 650	653, 717	0.050
9	425	555, 590	603, 653	0.154
10	420	515, 550, 590, 650	653, 717	0.200
11	425	555, 590	607, 653	0.183

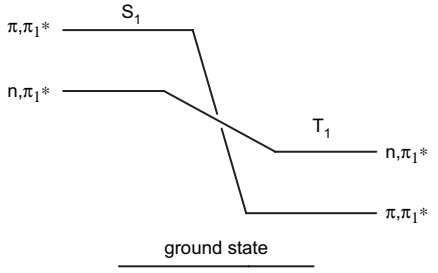

Fig. 5. Distribution of energy bands of S_1 and T_1.

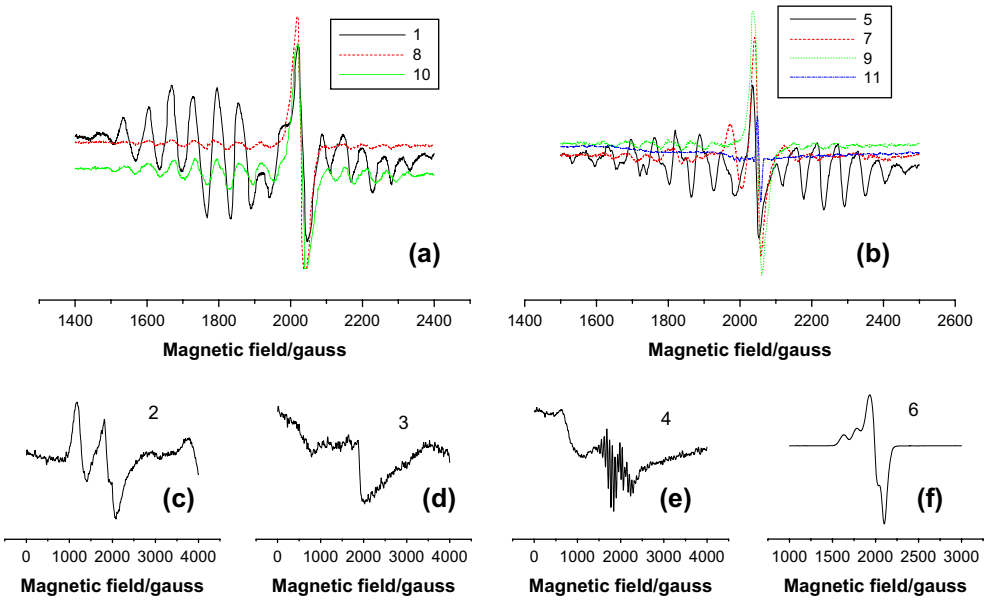

Fig. 6. EPR spectra of all porphyrin compounds.

The fluorescence quantum yields of the porphyrin compounds are listed in Table 1. Porphyrin **1**, which contained an electron-donating group displayed high quantum yield and **10**, for which S_1-S_1 energy transfer applied, also had high quantum yield. These findings may be of interest in the context of novel luminescence materials.

3.3. Electron paramagnetic resonance (EPR)

As mentioned, porphyrins have an extensive system of delocalized π electrons. The EPR signals of porphyrin compounds are generated by the interaction of the delocalized π electrons of the porphyrin or the unpaired electron of the metal ion with the magnetic field. The EPR spectra of the compounds were measured under different conditions, such as room temperature, low temperature (in liquid N_2 condition) and illumination. The experimental results showed that variations in these conditions had no effect on the spectra and so all measurements were carried out using solid samples at room temperature in the absence of illumination.

The EPR spectra of the metal-free porphyrins are shown in Fig. 6a. The hyperfine structure resulted from the interaction between delocalized π electron and N magnetic nuclei. Porphyrin **1** displayed the best response because of the presence of the OH group which resulted in an increase in the average electron density of the conjugated porphyrin system. As expected, **8**, in which an electron-withdrawing group was linked to the porphyrin macrocycle, showed the weakest response.

The EPR spectra of **7**, **9** and **11** are shown in Fig. 6b. In these three metalloporphyrins the central metal ions have no unpaired electron and so the mechanism of the appearance of the EPR signals was the same as that for the metal-free porphyrins. The hyperfine structures of these four types of metalloporphyrins were weaker than those of the corresponding metal-free porphyrins, and that of porphyrin **11** in which coordination with the two zinc ions could be barely seen. The EPR spectra of the metalloporphyrins **2**, **3**, **4**, **5** and **6** are shown in Fig. 6c, d, e, b and f, respectively. The EPR signals generated by unpaired electrons of the metal ion was very strong and masked the EPR signals generated by the delocalized π electron in **2**, **3** and **6**. Only the EPR spectrum of **4** showed signals generated by delocalized π electrons and the unpaired electron of Co^{2+}. Furthermore, the EPR spectrum of **5** showed that the signals generated by delocalized π electrons masked the signals generated by the unpaired electrons of Ni^{2+}.

4. Conclusions

A series of porphyrins and metalloporphyrins were synthesized and their UV–vis, fluorescence and EPR spectra were clearly influenced by differences in the peripheral substituents and the central transition metal ions. The fluorescence results provide potentially useful insight into the synthesis of novel luminescent materials while the EPR data could be of use in the context of novel EPR oximetry materials.

Acknowledgment

We thank the National Natural Science Foundation of China (No. 20071014) for financial support for this work.

References

[1] Lahtinen R, Fermín DJ, Kontturi K, Girault HH. Artificial photosynthesis at liquid/liquid interfaces: photoreduction of benzoquinone by water soluble porphyrin species. J Electroanal Chem 2000;483:81–7.
[2] Konishi Toshifumi, Ikeda Atsushi, Shinkai Seiji. Supramolecular design of photocurrent-generating devices using fullerenes aimed at modelling artificial photosynthesis. Tetrahedron 2005;61:4881–99.

[3] Rose E, Quelquejeu M, Pandian RP, Lecas-Nawrocka A, Vilar A, Ricart G, et al. Synthesis of porphyrins: models of natural hemoproteins and impressive catalysts for asymmetric epoxidation of olefins. Polyhedron 2000;19:581–6.
[4] Macdonald IJ, Dougherty TJ. Basic principles of photodynamic therapy. J Porphyrins Phthalocyanines 2001;5:105–29.
[5] Dudkowiak A, Teślak E, Habdas J. Photophysical studies of tetratolylporphyrin photosensitizers for potential medical applications. J Mol Struct 2006;792–793:93–8.
[6] Crossley MJ, Burn PL. An approach to porphyrin-based molecular wires: synthesis of a bis(porphyrin)tetraone and its conversion to a linearly conjugated tetrakisporphyrin system. J Chem Soc Chem Commun 1991;21:1569–71.
[7] Wagner RW, Lindsey JS. A molecular photonic wire. J Am Chem Soc 1994;116:9759–60.
[8] Kawao M, Ozawa H, Tanaka H, Ogawa T. Synthesis and self-assembly of novel porphyrin molecular wires. Thin Solid Films 2006;499:23–8.
[9] Ishida T, Morisaki Y, Chujo Y. Synthesis of covalently bonded nanostructure from two porphyrin molecular wires leading to a molecular tube. Tetrahedron Lett 2006;47:5265–8.
[10] Wrobel D, Lukasiewicz J, Goc J, Waszkowiak A, Ion R. Photocurrent generation in an electrochemical cell with substituted metalloporphyrins. J Mol Struct 2000;555:407–17.
[11] Guldi DM. J Phys Chem B 2005;109:11432–41.
[12] Hasobe T, Kamat PV, Troiani V, Solladie N, Ahn TK, Kim SK, et al. J Phys Chem B 2005;109:19–23.
[13] Takechi K, Shiga T, Motohiro T, Akiyama T, Yamada S, Nakayama H, et al. Solar cells using iodine-doped polythiophene–porphyrin polymer films. Solar Energy Mater Sol Cells 2006;90:1322–30.
[14] Anderson HL, Martin SJ, Bradley DDC. Synthesis and third-order nonlinear optical properties of a conjugated porphyrin polymer. Angew Chem Int Ed Engl 1994;33:655–7.
[15] Ogawa K, Zhang TQ, Yoshihara K, Kobuke Y. Large third-order optical nonlinearity of self-assembled porphyrin oligomers. J Am Chem Soc 2002;124:22–3.
[16] Screen TEO, Thorne JRG, Denning RG, Bucknell DG, Anderson HL. Amplified optical nonlinearity in a self-assembled double-strand conjugated porphyrin polymer ladder. J Am Chem Soc 2002;124:9712–3.
[17] Yang Li, Lifeng Cao, He Tian. Fluoride ion-triggered dual fluorescence switch based on naphthalimides winged zinc porphyrin. J Org Chem 2006;71:8279–82.
[18] Swartz HM, Clarkson RB. The measurement of oxygen *in vivo* using EPR techniques. Phys Med Biol 1998;43:1957–75.
[19] Dexter DL. A theory of sensitized luminescence in solid. J Chem Phys 1953;21:836–50.
[20] Shi YY, Zheng WQ, Li XQ, Yu LX, Wang XQ. Flourescence property of a series of hydroxylphenyl porphyrins. Chem J Chin Univ 2005;26:9–12.
[21] Fa HB, Zhao L, Wang XQ. Synthesis of a mesoporphyrin dimer by direct condensation between two moso-carboxy group of porphyrin ring. Chem J Chin Univ 2006;27:17–9.
[22] Kibbey CE, Meyehoff ME. Preparation and characterization of covalently bound tetraphenylporphyrin-silica gel stationary phases for reversed-phase and anion-exchange chromatography. Anal Chem 1993;65:2189–96.
[23] Shan N, Zheng WQ, Fa HB, Wang XQ. Metallization and characterization of meso-5-(*p*-hydroxyphyl)-10,15,20-triphenylporphyrin. J Jilin University (Science Edition) 2007;45(2):283–7.
[24] Kroon J, Oliver AM, Paddon-Row MN, Verhoeven JW. Observation of a remarkable dependence of the rate of singlet–singlet energy transfer on the configuration of the hydrocarbon bridge in bichromophoric systems. J Am Chem Soc 1990;112:4868–73.